Circulation

RESEARCH LETTER

Regulation of Postnatal Cardiomyocyte Maturation by an RNA Splicing Regulator RBFox1

Jijun Huang, PhD*; Josh Z. Lee, PhD*; Christoph D. Rau, PhD; Arash Pezhouman, MD; Tomohiro Yokota, PhD; Hiromi Miwa, PhD; Matthew Feldman, BA; Tsz Kin Kong, BS; Ziyue Yang, BS; Woan Ting Tay, BS; Ivan Pushkarsky, PhD; Kyungsoo Kim, PhD; Shan S. Parikh, MD, PhD; Shreya Udani, PhD; Boon Seng Soh, PhD; Chen Gao, PhD; Linsey Stiles, PhD; Orian S. Shirihai, MD, PhD; Bjorn C. Knollmann, MD, PhD; Reza Ardehali, MD, PhD; Dino Di Carlo, PhD; Yibin Wang, PhD

Cardiomyocyte maturation from neonatal to adult stage involves complex changes in myocyte morphology, proliferative capacity, metabolism, and physiology. However, the underlying regulatory mechanism remains poorly understood.[1,2] Whereas several extrinsic factors, such as mechanical load, electrical stimulation, hormones, and nutrients, have been implicated in this process,[2] the intrinsic regulatory circuit governing cardiomyocyte postnatal maturation is largely unknown. In search of answers, we analyzed the global transcriptome changes between neonatal and adult rat hearts.

Gene Ontology analysis from differentially expressed genes revealed expected changes in cell cycle, metabolism, and contractility. In addition, mRNA splicing was among the top enriched differentially expressed gene pathways, the functional significance of which in cardiomyocyte maturation is unreported (Figure [A]). Among the top cardiac enriched RNA splicing regulators, we found *Rbfox1* (RNA binding fox-1 homolog 1) showed a negligible level of expression in neonatal rat heart but was dramatically induced in adult rat heart[3] (Figure [B]). Examination of a previously published single-cell RNA sequencing (RNA-seq) dataset from postnatal (P1 to P14) mouse hearts[4] (Figure [C]) also revealed that Rbfox1 expression was low in perinatal hearts, but highly induced in a subpopulation of cardiomyocytes present predominantly in P14 hearts (Figure [D], top left), which also have the lowest expression of cell-cycle–related genes and the highest expression of genes associated with mature cardiomyocytes (Figure [D]). Ectopic expression of Rbfox1 in neonatal rat ventricular cardiomyocytes resulted in enlarged cell size (Figure [E]), elevated expression genes involved in calcium handling (*Ryr2*, *Atp2a2*, and *Pln*), metabolism (*Ckm*), and cell–cell coupling (*Cnx43*; Figure [F]), enhanced sarcomere organization (Figure [G] and [H]), and higher percentage of binucleation (Figure [I]). However, no significant effect on T-tubule formation was observed. In line with these molecular and morphologic features, Rbfox1-expressing cardiomyocytes showed more robust contraction (Figure [J] and [K]) and better maintained intracellular calcium transients measured by both time to peak and time to decay under 2 Hz pacing condition (Figure [L] and [N]). In addition, whole-field optical mapping showed significantly reduced action potential duration in Rbfox1-expressing neonatal rat ventricular cardiomyocytes (Figure [O] and [P]), a characteristic feature of electrophysiologic maturation in rodent cardiomyocytes. Rbfox1 expression also enhanced oxygen consumption in cardiomyocytes (Figure [Q]) without affecting mitochondrial content on the basis of mito-DNA to genomic DNA ratio (data not shown). In human pluripotent stem cell–derived cardiomyocytes, Rbfox1 expression was below detection. Ectopic expression of Rbfox1 significantly increased the expression of cardiac genes associated with maturation, including *MYH6*, *MYH7*, *SERCA2A*, and *CKM* (Figure [R]), and enhanced sarcomere organization (Figure [S] and [T]). At functional level, Rbfox1-expressing human

Key Words: myocytes, cardiac ■ RNA, messenger ■ sequence analysis, RNA

Correspondence to: Yibin Wang, PhD, Duke-NUS Medical School, 8 College Rd, Level 8, Singapore 169857, Singapore. Email yibinwang@duke-nus.edu.sg
*J. Huang and J.Z. Lee contributed equally.
For Sources of Funding and Disclosures, see page 1266.

Circulation is available at www.ahajournals.org/journal/circ

CORRESPONDENCE

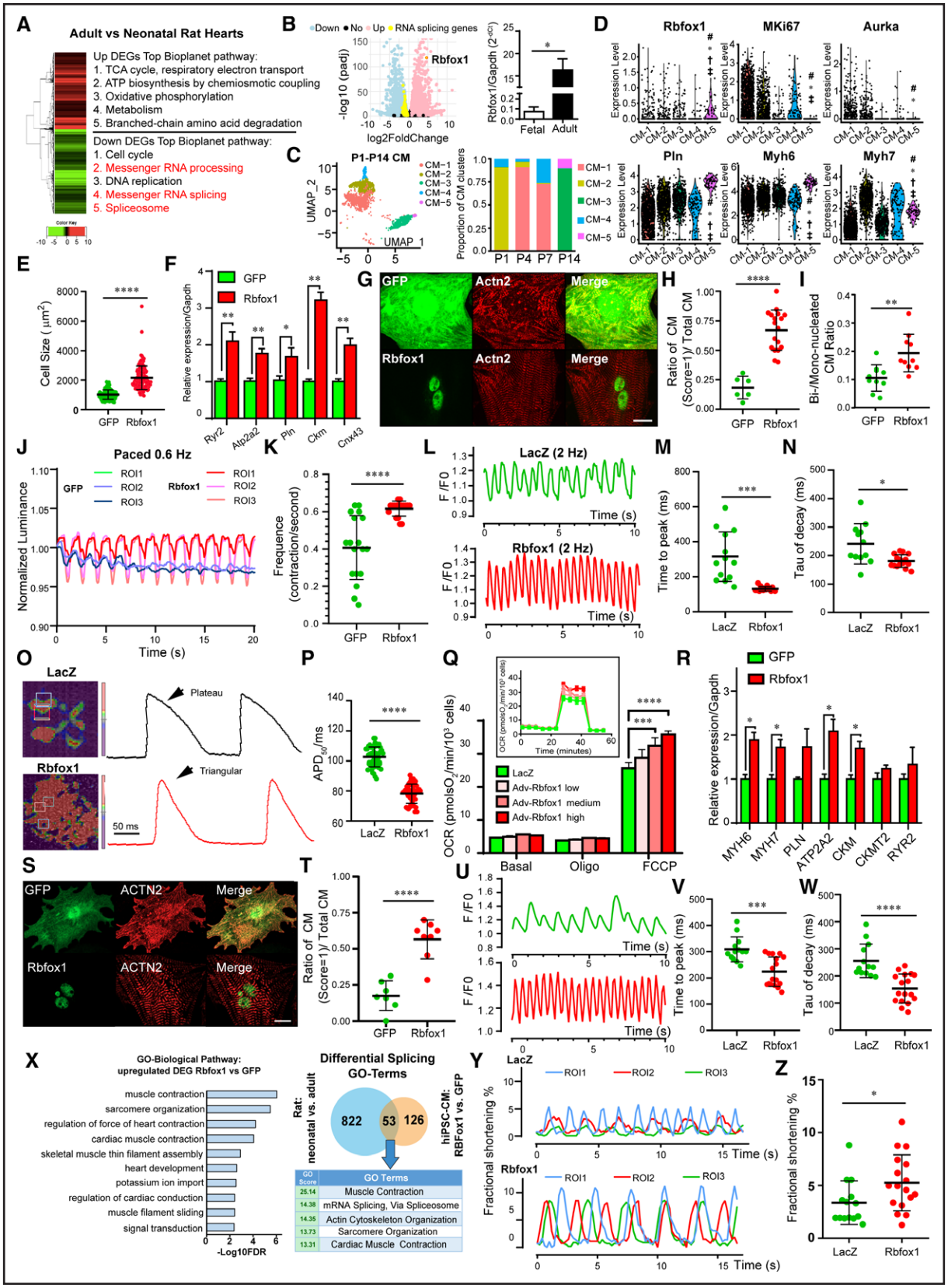

Figure. RBFox1 promotes rodent neonatal and human induced pluripotent stem cell–derived cardiomyocyte maturation at molecular, morphologic, and functional levels.

A, Top BioPlanet pathway terms enriched with upregulated or downregulated differentially expressed genes (DEGs) between adult versus neonatal rat heart on the basis of RNA sequencing (RNA-seq). **B**, Volcano plot showing *Rbfox1* and mRNA splicing pathway genes among all the DEGs in the RNA-seq data set from (**A**). DEGs cutoff, |log2FC|>0.5 and P_{adj}<0.05; Bonferroni correction was used to calculate (*Continued*)

Figure Continued. the adjusted *P* values. The insert bar graph shows expression of Rbfox1 measured by reverse transcription quantitative polymerase chain reaction (n=3, with 6 to 8 hearts pooled together for each n in the fetal samples; **P*<0.05; unpaired Welch *t* test). **C**, Left, Uniform manifold approximation and projection (UMAP) distribution of single-cell RNA-seq data showing P1 to P14 postnatal mouse cardiomyocytes (CMs) labeled by subclusters (CM1 through CM5); right, CM subcluster composition at each time point from P1 to P14. **D**, Violin plot showing expression of *Rbfox1*, cell cycle genes (*Mki67*, *Aurka*), and cardiac genes (*Pln*, *Myh6*, *Myh7*) scaled across different CM subclusters. Significance was labeled between CM5 and CM1 through CM4; statistical analysis was performed by Kruskal-Wallis test followed by Dunn multiple comparison in R. **E**, Cell size comparison of Rbfox1 versus green fluorescent protein (GFP)–expressing neonatal rat ventricular myocytes (NRVMs). *****P*<0.0001; Wilcoxon rank-sum test; each dot represents 1 cell. **F**, mRNA levels of Ca^{2+} handling genes in Rbfox1 versus GFP-expressing NRVMs (n=7; **P*<0.05; ***P*<0.01; 2-way ANOVA with Sidak multiple-comparisons test). **G**, Representative immunofluorescent staining of sarcomere protein ACTN2 (α-actinin-2) in NRVMs expressing GFP (top) or Rbfox1 (bottom; scale bar=20 μm). **H** and **I**, Ratio of NRVMs with sarcomere score=1 versus total number of NRVMs (**H**) and ratio of binucleated versus mononucleated cardiomyocytes (**I**) in NRVMs expressing GFP or Rbfox1. Sarcomere score=1, defined as cardiomyocytes with 50% or more cell body covered with aligned ACTN2 staining. Each data point represents the average value from an imaging field; each field contained 7 to 21 cells (**H**) or 20 to 40 cells (**I**; ***P*<0.01; *****P*<0.0001; unpaired Student *t* test; data passed normality test and variance is equal). **J** and **K**, Myocyte contraction on the basis of edge-tracing and beating frequency from NRVMs expressing GFP or Rbfox1 under electrical pacing at 0.6 Hz. Representative contraction curve from 3 regions of interest (ROIs; **J**). Quantitative frequency in GFP versus the Rbfox1 group (**K**; *****P*<0.0001; Wilcoxon rank-sum test, dots represent individual ROIs). **L**, Cytosolic Ca^{2+} transients in NRVMs expressing LacZ or Rbfox1 at a pacing frequency of 2.0 Hz measured with Fluo3-AM. **M** and **N**, Kinetics of calcium transients: time to peak (**M**) and tau of decay (**N**). Data were summarized from 2 independent experiments (**P*<0.05; ****P*<0.001; unpaired Welch *t* test). **O**, Action potential profile in LacZ (control; top) and Rbfox1-expressing NRVMs (bottom) measured by whole-field optical imaging. FluoVolt Membrane Potential Kit was used as the action potential dye. **P**, Action potential duration as measured at time to 50% decay (APD_{50}; n=50 ROIs from 3 independent sets; *****P*<0.0001; unpaired Student *t* test; data passed normality test and variance is equal). **Q**, Oxygen consumption rate (OCR) in NRVMs expressing LacZ or increasing levels of Rbfox1 after adv-Rbfox1 infection at low (5.37×10^7 opu/mL), medium (1.34×10^8 opu/mL), and high (2.68×10^8 opu/mL) titers (****P*<0.001; *****P*<0.0001; 5 replicates in each time point; 2-way ANOVA with Sidak correction of multiple comparison; 2 factors were groups [LacZ, Adv-Rbfox1] and mitochondrial status [basal, oligomycin, FCCP]). **R**, Expression of Ca^{2+} handling and cardiomyocyte maturation genes in Rbfox1- versus GFP-treated human induced pluripotent stem cell–derived cardiomyocytes (hiPSC-CMs; **P*<0.05; from 3 biological repeats; unpaired Student *t* test). **S**, Representative immunofluorescent image of hiPSC-CM–expressing GFP (top) or Rbfox1 (bottom) for sarcomere protein ACTN2 (scale bar=20 μm). **T**, Ratio of sarcomere score=1 hiPSC-CM versus total number of cells in each image field; each field contained 5 to 25 cells (*****P*<0.0001; unpaired Student *t* test; data passed normality test and variance is equal). **U**, Calcium transients in hiPSC-CM–expressing LacZ (control) or Rbfox1 (frequency=2.0 Hz). **V** and **W**, Kinetics of calcium transients: time to peak (**V**) and tau of decay (**W**; data were summarized from 2 independent experiments; ****P*<0.001; *****P* < 0.0001; Wilcoxon rank-sum test). **X**, Top enriched Gene Ontology (GO) terms in DEGs (left) and Rbfox1-regulated and cardiomyocyte maturation–associated RNA splicing genes between neonatal versus adult rat heart and hiPSC-CMs expressing Rbfox1 versus GFP (right). **Y**, Representative traces of FLECS (fluorescently labeled elastomeric contractible surfaces) constructs under spontaneous contraction seeded with hiPSC-CM–expressing LacZ (top) or Rbfox1 (bottom). Three individual ROIs are shown. **Z**, Fractional shortening of FLECS constructs seeded with hiPSC-CM–expressing Rbfox1 versus LacZ (**P*<0.05; Wilcoxon rank-sum test; each dot represents an individual patterned contraction unit; all error bars represent SD).

induced pluripotent stem cell–derived cardiomyocytes showed sustained pacing-matched calcium transients at 2 Hz pacing frequency compared with mismatched calcium transients observed in the control cells (Figure [U]). Rbfox1-expressing myocytes showed robust calcium cycling with shorter time to peak and time to decay (Figure [V] and [W]). Transcriptome profiling by RNA-seq followed by Gene Ontology enrichment analysis (Figure [X], left) showed that Rbfox1 led to differentially expressed genes enriched in cardiac muscle contraction, sarcomere organization, and cardiac conduction, and differential RNA splicing in genes enriched in cardiac contraction and sarcomere structure (Figure [X], right). Using a patterned elastomeric sensor platform (FLECS [fluorescently labeled elastomeric contractible surfaces][5]), we directly measured contractile performance of human induced pluripotent stem cell–derived cardiomyocytes upon Rbfox1 expression and observed more robust contractility compared with the LacZ-expressing controls (Figure [Y] and [Z]).

Bulk RNA-seq data from rat hearts and human induced pluripotent stem cell–derived cardiomyocytes are publicly available at the National Center for Biotechnology Information Sequence Read Archive database and can be accessed with Sequence Read Archive BioProject IDs PRJNA295071 (rats) and PRJNA932451 (human induced pluripotent stem cell–derived cardiomyocytes). The single-cell RNA-seq data were obtained from GEO database GSE122706. Other data and materials that support the findings of this study are available from the corresponding author upon reasonable request.

The following software was used: Seurat 4.0.2 for the single-cell RNA-seq dataset, Salmon 0.8.2 for the bulk RNA-seq data, DESEQ2 for differentially expressed gene analysis, GeneAnalytics Suite and Enrichr for pathway analysis, ggPlot2 v3.3.5 for volcano plot, zCardio v1.0.8 for contraction analysis, Clampfit 11.2 for calcium analysis, SiMedia 2030 BV Analyze for optical mapping, ImageJ v1.5.3A for FLECS data, and GraphPad Prism 8 and R package dunn.test for statistical analysis. All the animal and human induced pluripotent stem cell–derived cardiomyocyte studies were approved by the institutional protocol ARC-2003-105 and hPSCRO 2017-002-07 at the University of California, Los Angeles.

Rbfox1-mediated mRNA splicing is part of molecular changes during myocyte postnatal maturation. Its expression is sufficient to promote rodent neonatal and human induced pluripotent stem cell–derived cardiomyocyte

maturation at molecular, morphologic, and functional levels. Although this is the first proof-of-concept evidence that RNA-splicing regulation can significantly affect cardiomyocyte maturation, the expression of RBFox1 alone is not sufficient to mature cardiomyocytes to full adult stage, including T-tubule formation. Nevertheless, this study offers new insight into myocyte maturation regulatory network by uncovering an intrinsic post-transcriptional circuit in this process. Its application in disease modeling and cell-based therapy, as well as the underlying mechanism linking RBFox1-mediated RNA splicing and downstream maturation processes, needs further exploration.

ARTICLE INFORMATION

Affiliations

Cardiovascular Laboratory, Division of Molecular Medicine, Department of Anesthesiology and Perioperative Medicine (J.H., J.Z.L., C.D.R., T.Y., T.K.K., C.G., Y.W.), Division of Endocrinology (J.H.), Department of Medicine, David Geffen School of Medicine (L.S., O.S.S.), Division of Cardiology, Department of Medicine (A.P., T.Y., R.A.), and Department of Bioengineering, Samueli School of Engineering (H.M., S.U., D.D.), University of California, Los Angeles. Department of Genetics and Computational Medicine, University of North Carolina, Chapel Hill (C.D.R.). Department of Medicine, Greater Los Angeles VA Healthcare System, CA (T.Y.). School of Medicine, Meharry Medical College, Nashville, TN (M.F.). Department of Molecular and Cellular Biology, Baylor College of Medicine, Houston, TX (Z.Y.). Forcyte Biotechnologies, Inc, Los Angeles, CA (I.P.). Vanderbilt Center for Arrhythmia Research and Therapeutics, Department of Medicine, Vanderbilt University School of Medicine, Nashville, TN (K.K., S.S.P., B.C.K.). Institute of Molecular and Cell Biology, The Agency for Science, Technology and Research (A*STAR), Singapore (B.S.S.). Department of Pharmacology and System Physiology, University of Cincinnati, OH (C.G.). Section of Cardiology, Department of Internal Medicine, Baylor College of Medicine, Houston, TX (A.P., R.A.). Signature Research Program of Cardiovascular and Metabolic Diseases, Duke-NUS Medical School, Singapore (W.T.T., Y.W.).

Acknowledgments

The authors thank the Technology Center for Genomics & Bioinformatics Core, The Mitochondrial and Metabolism Core, and the Neonatal Rodent Cardiomyocyte Core at the University of California, Los Angeles; Dr Adam Langenbacher and Dr Jau-Nian Chen at the University of California, Los Angeles, for assistance with software use in cardiomyocyte contraction analysis; Dr Zhengyi Zhang at the University of California, Los Angeles, for technical support in bioinformatic analysis; Dr Joseph C. Wu at the Stanford Cardiovascular Institute iPSC Biobank for providing human induced pluripotent stem cell–derived cardiomyocytes; Dr Long-Sheng Song at the University of Iowa for sharing T-tubule staining dye; and Haiying Pu and Yea-Len Park for support with animal management.

Sources of Funding

This work was supported by American Heart Association Postdoctoral Award 18POST33990469 to Dr Huang, National Institutes of Health grants R01 HL148714 to Dr Ardehali and R00 HL141626 to Dr Gao, and Department of Defense Award PR171540 to Dr Wang.

Disclosures

None.

REFERENCES

1. Karbassi E, Fenix A, Marchiano S, Muraoka N, Nakamura K, Yang X, Murry CE. Cardiomyocyte maturation: advances in knowledge and implications for regenerative medicine. *Nat Rev Cardiol*. 2020;17:341–359. doi: 10.1038/s41569-019-0331-x
2. Guo Y, Pu WT. Cardiomyocyte maturation: new phase in development. *Circ Res*. 2020;126:1086–1106. doi: 10.1161/CIRCRESAHA.119.315862
3. Gao C, Ren S, Lee JH, Qiu J, Chapski DJ, Rau CD, Zhou Y, Abdellatif M, Nakano A, Vondriska TM, et al. RBFox1-mediated RNA splicing regulates cardiac hypertrophy and heart failure. *J Clin Invest*. 2016;126:195–206. doi: 10.1172/JCI84015
4. Wang Y, Yao F, Wang L, Li Z, Ren Z, Li D, Zhang M, Han L, Wang SQ, Zhou B, et al. Single-cell analysis of murine fibroblasts identifies neonatal to adult switching that regulates cardiomyocyte maturation. *Nat Commun*. 2020;11:2585. doi: 10.1038/s41467-020-16204-w
5. Pushkarsky I. FLECS technology for high-throughput single-cell force biology and screening. *Assay Drug Dev Technol*. 2018;16:7–11. doi: 10.1089/adt.2017.825